2

Nanofiber Reinforced Composite Polymer Electrolyte Membranes

A. Kumar and M. Deka
Department of Physics, Tezpur University, Tezpur784028, Assam India

1. Introduction

The path breaking studies of Wright and Armand on ionically conducting polymers, called "polymer electrolytes" in the 1970s have opened an innovative area of materials research with potential applications in the power sources industry (Fenton et al., 1973). The main applications of the polymer electrolytes are in rechargeable lithium batteries as an alternative to liquid electrolytes (Chen et al., 2002; Lobitz et al., 1992). The advantages such as no leakage of electrolyte, higher energy density, flexible geometry and improved safety hazards have drawn the attention of many researchers on the development of lithium polymer batteries and other electrochemical devices such as supercapacitors, electrochromic windows, and sensors (Gray, 1991). In batteries being a separator membrane polymer electrolyte must meet the following requirements.

1. high ionic conductivity
2. high cationic transference number
3. good dimensional stability
4. high electrochemical stability and chemical compatibility with both Li anode and cathode material and
5. good mechanical stability.

The need for high ionic conductivity arises from the fact that at what rate or how fast energy from a Li-battery can be drained, which largely depends on the extent of ionic mobility in the electrolyte and hence on ionic conductivity. For battery applications, along with high ionic conductivity the electrolyte material must be dimensionally stable since the polymer electrolyte will also function as separator in the battery, which will provide electrical insulation between the cathode and the anode. This implies that it must be possible to process polymer electrolyte into freestanding film with adequate mechanical strength. Requirement of high cationic transport number rather than anionic is also important in view of the battery performance because concentration gradients caused by the mobility of both cations and anions in the electrolyte arise during discharging, which may result in premature battery failure.

Recent advances in nanotechnology have made materials and devices easier to be fabricated at the nanoscale. Nanofibres and nanowires with their huge surface area to volume ratio, about a thousand times higher than that of a human hair, have the potential to significantly improve current technology and find applications in new areas. Nanofibers in particular,

Source: Nanofibers, Book edited by: Ashok Kumar,
ISBN 978-953-7619-86-2, pp. 438, February 2010, INTECH, Croatia, downloaded from SCIYO.COM

have been used for a wide range of applications such as tissue engineering (Bhattarai et al., 2004), filter media (Suthar & Chase, 2001), reinforcement in composites (Chatterjee & Deopura, 2002) and micro/nano-electro-mechanical systems (MEMS/NEMS) (Sundararajan et al., 2002). Such fibers can be made from various materials such as polymers, carbon and semiconductors into the form of continuous nanofibers, nanofibrous networks or short nanowires and nanotubes. On the other hand polymer nanocomposite formation through the reinforcement of particles having dimensions less than 100 nm into polymer matrix finds important applications for the development of advanced materials. This reinforcement occurs for particles of spherical shape as well as for plate-like and fibrous nanofillers, the latter with their high aspect ratio exhibits a stronger effect. As a result, nanofibers because of their excellent mechanical properties coupled with very high aspect ratio theoretically are the ideal candidates for reinforcing a polymer matrix. The main challenge in this case lies in the fact of increased specific surface area due to the small size of the reinforcing particles, forces per unit mass resulting from interactions between this surface and surrounding area become more pronounced. As a result nanofibers cannot be easily dispersed in substances of different surface energy. However a strong interface between the reinforcing phase and the host matrix is always desirable in order to achieve desirable properties.

2. Types of polymer electrolytes

The development of polymer electrolytes has passed mainly three stages namely: (a) solid polymer electrolytes, (b) gel polymer electrolytes and (c) composite polymer electrolytes. In dry solid polymer electrolytes the polymer host itself is used as a solid solvent along with lithium salt and does not contain any organic liquids. The most commonly studied polymer electrolyte membranes are complexes of Li salts with a high molecular weight polyethylene oxide (PEO) (Ahn et al., 2003). PEO excels as a polymer host because of its high solvating power for lithium ions and its compatibility with the lithium electrode (Algamir & Abraham, 1994). However, it is also known that the high conductivity (10^{-3}-10^{-4} S/cm) of most PEObased polymer electrolytes requires operation in the temperature range of 80-100 °C (Ahn et al., 2003; Algamir & Abraham, 1994; Abraham, 1993; Kovac et al., 1998), below which these electrolytes suffer from low conductivity values in the range of 10^{-7}-10^{-8} S/cm because of the high crystallinity of PEO (Kovac et al., 1998). Gel electrolytes are formed by incorporating an electrolyte solution into polymer matrix (Algamir & Abraham, 1994; Tarascon et al., 1996). Since the electrolyte molecules such as ethylene carbonate (EC), propylene carbonate (PC), diethyl carbonate (DEC) can solvate ions, coordinating polymers like PEO are no longer necessary. The ion conduction in these electrolytes takes place through the liquid electrolytes where the host polymer mostly provides the structural support. The gel polymer electrolyte systems based on poly(methyl methacrylate) (PMMA) (Rajendran & Uma, 2000; Rajendran et al., 2001; Stephan et al., 2000; Feuillade & Perche, 1975) have been proposed for lithium battery application particularly because of their beneficial effects on stabilization of the lithium–electrolyte interface (Appetecch et al., 1995). However, reasonable conductivity achieved of such plasticized film is offset by poor mechanical properties at high plasticizer content. Rajendran et al. (Rajendran & Uma, 2000; Rajendran et al., 2001) were able to improve the mechanical property of PMMA by blending with poly(vinyl alcohol) (PVC). However, a decrease of ionic conductivity was observed due to higher viscosity and lower dissociability of lithium salt. Recently poly(vinylidenefluoride) (PVdF) as a host has drawn the attention of many researchers due to its high anodic stability

and high dielectric constant (ε = 8.4) which helps in greater ionization of lithium salts (Choe et al., 1995). Unfortunately, PVdF-based polymer electrolytes suffer due to syneresis; a phenomenon by which the liquid component separates out from the host matrix in due course or upon application of pressure leading to battery leak and related safety problems. Very recently, poly(vinylidenefluoride-co-hexafluoropropylene) {P(VdF-HFP)} based systems have drawn the attention of many researchers because of its various appealing properties like high dielectric constant, low crystallinity and glass transition temperature (Song et al., 2000; Wu et al., 2006; Stephan et al., 2006; Stephan & Nahm, 2006; Stolarska et al., 2007; Michael & Prabaharan, 2004). P(VdF-HFP) has excellent chemical stability due to VdF unit and plasticity due to HFP unit (Aravindan & Vickraman, 2007). However, gelled or plasticized P(VdF-HFP) based electrolytes exhibit drawbacks, such as increased reactivity with lithium metal electrode, solvent volatility and poor mechanical properties at high degree of plasticization (Jacob et al., 2003). In order to retain the mechanical properties of polymer gel electrolytes, the gel films have to be hardened either by chemical or physical curing (high energy radiation), which results in high processing costs. Alternatively, the addition of inert oxides to the polymer electrolytes has recently become an ever increasing attractive approach, due to the improved mechanical stability, enhanced ionic conductivity and electrode-electrolyte interface stability (Croce et al., 1998; Quartarone et al., 1998). This type of electrolyte is known as composite polymer electrolyte. The increase in ionic conductivity in composite polymer electrolytes depends on the concentration and particle size of the inert solid phases. Generally, smaller the particle sizes of the oxides, the larger the conductivity enhancement. However, due to the absence of exact structure–property correlations in the polymer electrolyte systems, a complete understanding of the ion conduction phenomenon is still lacking. Nonetheless, to explain the mechanistic aspects of ion transport in micro/nanocomposite polymer electrolyte systems, a working hypothesis has been suggested accordingly to which, the dispersion of submicron or nano-size filler particles having large surface area, into the polymer host lowers the degree of crystallinity, which may also be thought to be due to Lewis acid–base interaction between ceramic surface states and polymer segments (Croce et al., 1998; Golodnitsky et al., 2002). Hence, in addition to the usual space charge effects of the dispersoid particles, the increased amorphosity would also support the conductivity enhancement in terms of increased ionic mobility through the amorphous phase. Essentially because of this idea, nanocomposite polymer electrolytes wherein nanosized inert solid particles are added to the polymer electrolytes are presently the focus of many studies, both practical as well as theoretical.

It has been reported that addition of nanoscale inorganic fillers, such as alumina (Al_2O_3), silica (SiO_2), titania (TiO_2) etc. to the polymer electrolytes resulted in the improvements of transport properties as well as mechanical and electrochemical properties (Kim et al., 2001; Kim et al., 2002; Scrosati et al., 2000). A novel composite micro-porous polymer electrolyte membrane based on optimized composition of P(VdF-HFP)-ZrO_2 was prepared by a preferential polymer dissolution process. The incorporation of ZrO_2 nanoparticles in the P(VdF-HFP) matrix, improved the ionic conductivity due to the availability of a large amount of oxygen vacancies on ZrO_2 surface which may act as the active Lewis acidic sites that interact with ions (Kalyana et al., 2007). A gel polymer electrolyte based on the blend of poly(methyl methacrylate-co-acrylonitrile-co-lithium methacrylate) (PMAML) and poly(vinylidene fluoride-co-hexafluoropropylene) P(VdF-HFP)) was prepared and characterized. The highest ionic conductivity achieved in the system was 2.6×10^{-3} S cm $^{-1}$ at

ambient temperature (Wang & Tang, 2004). Highly conducting porous polymer electrolytes comprised of P(VdF-HFP), metal oxide (TiO_2, MgO, ZnO)/or mesoporous zeolite (MCM-41, SBA-15), ethylene carbonate (EC), propylene carbonate (PC) and $LiClO_4$ were fabricated with a simple direct evaporation method. These polymer composite electrolytes were stable up to 5.5 V (versus Li/Li^+) and the lithium ion cells assembled with these polymer electrolytes show a good performance at a discharge rate below $C/2$ (Wu et al., 2006). Composite polymer electrolyte (CPE) membranes, comprising P(VdF-HFP), aluminum oxyhydroxide ($AlO[OH]_n$) of two different sizes 7 μm/14 nm and $LiN(C_2F_5SO_2)_2$ as the lithium salt were prepared using a solution casting technique. The incorporation of nanofillers greatly enhanced the ionic conductivity and the compatibility of the composite polymer electrolyte (Stephan et al., 2006). Nano SiO_2–P(VDF-HFP) composite porous membranes were prepared as the matrix of porous polymer electrolytes through *in situ* composite method based on hydrolysis of tetraethoxysilane and phase inversion. It is found that the *in situ* prepared nano silica was homogeneously dispersed in the polymeric matrix, enhanced conductivity and electrochemical stability of porous polymer electrolytes, and improved the stability of the electrolytes against lithium metal electrodes (He et al., 2005). Composite polymer membranes comprising of P(VdF-HFP) /Al_2O_3 were prepared by phase inversion technique with poly(ethylene glycol) (PEG) as an additive. The polymer membrane prepared with a weight ratio of PVdF-HFP (40):PEG (40):Al_2O_3 (20) showed maximum protonic conductivity due to the combined effect of inert filler and its porous nature (Kumar et al., 2007). The protonic conductivity of silica polymerized *in situ* within a P(VdF-HFP) matrix has been studied. The conductivity linearly increases with the silica content (Carrière et al., 2001). Gel polymer electrolyte membranes composed of P(VdF-HFP) and surface modified aluminum or titanium oxide were prepared according to the so-called Bellcore process. The ionic conductivity of polymer membrane increased by more than one order of magnitude upon the addition of filler into polymer host (Stolarska et al., 2007). Nanocomposite polymer electrolyte (NCPE) membranes of P(VdF-HFP) matrix with ethylene carbonate and diethyl carbonate mixtures as plasticizing agents, SiO_2 nanoparticles as filler and complexed with $LiPF_3(CF_3CF_2)_3$ were prepared by solvent casting technique. NCPE membranes containing 2.5 wt% of SiO_2 exhibited enhanced conductivity of 1.13 mS cm^{-1} at ambient temperature (Arvindan & Vickraman, 2007). Various amounts of nanoscale rutile TiO_2 particle were used as fillers in the preparation of P(VdF-HFP)-based porous polymer electrolytes. Physical, electrochemical and transport properties of the electrolyte films were investigated in terms of surface morphology, thermal and crystalline properties, swelling behavior after absorbing electrolyte solution, chemical and electrochemical stabilities, ionic conductivity, and compatibility with lithium electrode (Kim et al., 2003).

In the present chapter we report novel composite polymer electrolytes by incorporating dedoped (insulating) polyaniline nanofibers instead of nanoparticles into P(VdF-HFP)-(PC+DEC)-$LiClO_4$ gel polymer electrolyte system and PEO-P(VdF-HFP)-$LiClO_4$ blend electrolyte system. The concentration of dedoped polyaniline nanofibers has been varied and its effects on ionic transport in both the systems have been investigated.

3. Synthesis techniques of nanofibers

3.1 Electrospinning

Electrospinning has been recognized as an efficient technique for the fabrication of polymer nanofibers. Various polymers have been successfully electrospun into ultrafine fibers in

recent years mostly in solvent solution and some in melt form. In terms of the flexibility of the process, electrospinning is able to fabricate continuous nanofibres from a huge range of materials. Of the major classes of materials, electrospinning is able to produce nanofibres of polymers, composites, semiconductors and ceramics (Huang et al., 2003; Chronakis, 2005). The formation of nanofibers through electrospinning is based on the uniaxial stretching of a viscoelastic solution. There are basically three components in a eletrospun setup: a high voltage power supply, a capillary tube with a needle and a metal collector. A typical electrospinning set up is shown in Fig. 1. When a sufficiently high voltage is applied to a liquid droplet, the body of the liquid becomes charged, and electrostatic repulsion counteracts the surface tension and droplet is stretched, at a critical point a stream of liquid erupts from the surface. This point of eruption is known as the Taylor cone (Taylor, 1969). If the molecular cohesion of the liquid is sufficiently high, stream breakup does not occur (if it does, droplets are electrosprayed) and a charged liquid jet is formed. As the jet dries out in flight, the mode of current flow changes from ohmic to convective as the charge migrates to the surface of the fibre. The jet is then elongated by a whipping process caused by electrostatic repulsion initiated at small bends in the fibre, until it is finally deposited on the grounded collector. The elongation and thinning of the fibre resulting from this bending instability leads to the formation of uniform fibres with nanometer-scale diameters (Li & Xia, 2004). The main advantage of the electrospinning nanomanufacturing process is that it is cost effective compared to that of most bottom-up methods. The nanofibers prepared from Electrospinning process are often uniform and continuous and do not require expensive purification unlike submicrometer diameter whiskers, inorganic nanorods and

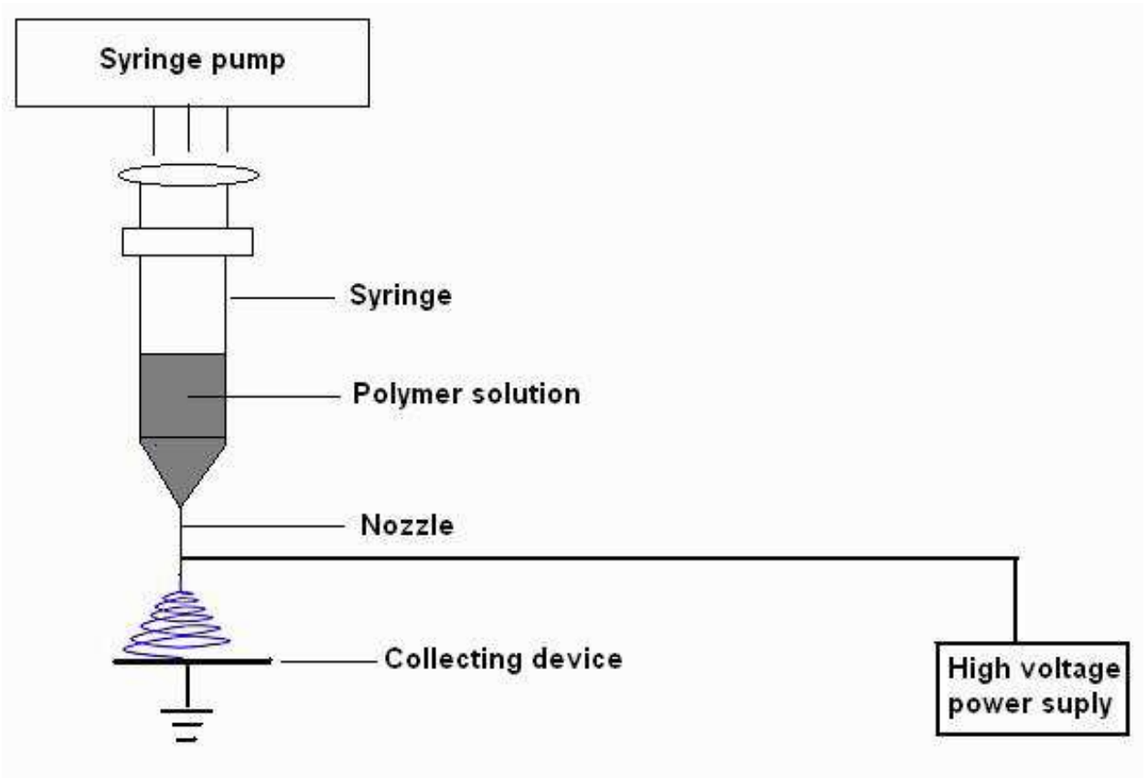

Fig. 1. Shematic diagram of electrospinning setup

carbon nanotubes (Dzenis, 2004). Polymer nanofibers mats are being considered for use in composite materials reinforcement, sensors, filtration, catalysis, protective clothing, biomedical applications, space applications such as solar cells, and micro- and nano optoelectronic device such as LEDs and photocells. Carbon nanofibers made from polymeric precursors further expand the list of possible uses of electrospun nanofibers (Li & Xia, 2004; Subbiah et al., 2005).

3.2 Template synthesis

An effective way to produce nanometer fibers (or nano-tubes) is based on the use of membrane-template techniques (Martin, 1961; Delvaux et al., 2000; Steinhart et al., 2002). Membranes, with nanochannels generated by fission-fragment tracks or by electrochemical etching of aluminum metal, are used as templates for either chemical or electrochemical deposition of conductive polymers (Pathasarathy & Martin, 1994), metal (Van de Zande et al., 1997), semiconductor (Klein et al., 1993), and other materials for the generation of nanofibers or nanotubes. Since the nanochannels on membranes are very uniform in size, the diameter and the aspect ratio of the nanofibers synthesized by the membranetemplate technique can be precisely controlled. This greatly facilitates the interpretation of optical data and the processing of these fibers (or tubes) into 2-D nanostructured materials (de Heer et al., 1995). Single-crystal semiconductor nanofibers can also be grown catalytically by metallorganic vapor phase epitaxy and laser ablation vapor-liquid-solid techniques (Morales & Lieber, 1998). The synthesis of these one-dimensional structures with diameters in the range of 3 to 15 nm holds considerable technological promise for optoelectronic device applications.

3.3 Phase separation

This method is normally used to synthesisze the polymer nanofibers. In phase separation, a polymer is first mixed with a solvent before undergoing gelation. The main mechanism in this process is the separation of phases due to physical incompatibility. One of the phase – which is that of the solvent – is then extracted, leaving behind the other other phase. In nutshell phase separation technique involves five basic steps (Ma & Zhang, 1999)

i. Dissolution of polymer.
ii. Liquid–liquid phase separation process.
iii. Polymer gelation (controls the porosity of nanoscale scaffolds at low temperature).
iv. Extraction of solvent from the gel with water.
v. Freezing and freeze-drying under vacuum.

Gelation is the most critical step that controls the porous morphology of the nanofibrous foams. The duration of gelation vary with polymer concentration and gelation temperature. At low gelation temperature nanoscale fiber networks are formed, whereas high gelation temperature results in the formation of a platelet-like structure due to the nucleation of crystals and their growth. This formation of platelet-like structure is overcome by increasing the cooling rates, which produce uniform nanofibers. However, gelation condition or polymer concentration does not affect the average diameter of fibers significantly. An increase in polymer concentration results in the decrease of porosity and increase of mechanical properties (Young's modulus and tensile strength). Other process parameters such as types of polymer and solvent, and thermal treatment also influence the morphology of the nanofibrous scaffolds (Zhang et al, 2005). The advantage of the phase separation

process is that it is a relatively simple procedure and the requirements are very minimal in terms of equipment compared with the previously discussed techniques of electrospinning and template synthesis.

3.4 Interfacial polymerization

Another effective and versatile way to synthesize nanofibers of conductive polymers is the interfacial polymerization technique. Generally conductive polymers like polyaniline, polypyrrole, PEDOT etc. are synthesized by this technique. This method was originally developed by Huang (Huang, 2003), where they synthesized nanofibers of polyaniline (PAni). Interfacial polymerization does not depend on any specific template or dopant. Highquality polyaniline nanofibers are obtained even when common mineral acids such as hydrochloric, sulfuric and nitric acids are used as dopants. They found it is the nature for PANI to form nanofibrillar morphology. In order to obtain pure PANI nanofibers, the secondary growth of the initially formed nanofibers must be suppressed. The interfacial polymerization of PAni involves the polymerization of aniline at the interface between two immiscible liquids, where the newly formed PAni nanofibers diffuse away from the interface to the aqueous solution because of their hydrophilic nature. This makes more reaction sites available at the interface and avoids further growth of the PAni nanofibers. S. Goel et. al. (Goel et al., 2007) reported the synthesis of polypyrrole nanofibers in the presence of different dopants including hydrochloric acid (HCl), ferric chloride (FeCl3), ptoluene sulfonic acid (p-TSA), camphor sulfonic acid (CSA), and polystyrene sulfonic acid (PSSA) using a simple interfacial oxidative polymerization method. They observed that that the electrical conductivity of PPy nanostructures depends upon the nature of dopant (PPy-p-TSA > CSA > HCl > FeCl3 > PSSA), PPy-p-TSA nanofibers showing the highest electrical conductivity of 6×10^{-2} S/cm.

4. P(VdF-HFP)-(PC+DEC)-$LiClO_4$-Dedoped polyaniline nanofibers composite gel polymer electrolyte system:

4.1 Preparation

The host copolymer poly(vinylidenefluoride-co-hexafluoropropylene) {P(VdF-HFP)} ($M_w \approx 400000$) and salt lithium perchlorate ($LiClO_4$) were received from Aldrich, USA.

These two raw materials were heated at 50° C and 100° C respectively before use to remove the moisture. Organic solvents propylene carbonate (PC) and diethyl carbonate (DEC) were used without further treatment as obtained from EMerck. Dedoped polyaniline (PAni) nanofibers were synthesized by the interfacial polymerization technique (Huang, 2006). The interfacial polymerization reaction was carried out in 30ml glass vials. 1M amount of aniline was dissolved in 10ml of organic solvent carbon tetrachloride (CCl_4). Ammonium peroxydisulfate {$(NH_4)_2S_2O_8$} (0.25M) was dissolved in 10 ml of double distilled water and dopant acid (HCl). The polyaniline nanofibers were dedoped with 1M NaOH. The electronic conductivity of PAni nanofibers was measured with Keithley 2400 LV souecemeter. The electronic conductivity of doped nanofibers is of the order of 10^{-4} Scm^{-1}, whereas after dedoping with NaOH solution the electronic conductivity was found to be of the order of 10^{-11} Scm^{-1}. This confirms the insulating nature of dedoped polyaniline nanofibers.

P(VdF-HFP)-(PC+DEC)-$LiClO_4$ - x wt. % dedoped PAni nanofiber (x= 0, 2, 4, 6, 8,10) membranes were prepared by conventional solution casting technique. Predetermined amounts of P(VdF-HFP), $LiClO_4$ and (PC+DEC) were dissolved in acetone in the ratio of

6:1.5:1.5:1 (by weight). Subsequently the solution was stirred at 50°C for 12 hours. PC has high dielectric constant (ε = 64.6) but has high viscosity (η = 2.53), whereas DEC has low dielectric constant (ε = 2.82) but has low viscosity (η = 0.748). Combination of PC and DEC (1:1 by volume) solvent was used as optimization for high dielectric constant (ε = 33.71) and low viscosity (η = 1.639) to achieve high ionic conductivity. After 12 hours of mixing at 50°C the dedoped polyaniline nanofiber was added in the gel polymer solution and allowed to stir for another 12 hours. The viscous solution thus obtained was cast onto Petri dish and allowed to dry at room temperature. Different membranes were synthesized by varying the concentration of dedoped polyaniline nanofibers.

The ionic conductivity of the nanocomposite polymer electrolyte films was determined by ac impedance measurements using a Hioki 3532-50 LCR Hitester in the frequency range from 42 Hz to 5MHz. The temperature dependence of ionic conductivity was also measured by heating the samples from room temperature (25°C) to 60°C. The nature of conductivity of nanofibers dispersed gel polymer electrolytes was determined by transference number measurements using Wagner polarization technique with polymer electrolyte membrane between graphite blocking electrodes. The transference number was found to be = 0.98 indicating that conductivity was essentially ionic in nature. The interfacial stability of nanocomposites polymer electrolytes was studied by fabricating stainless steel/polymer electrolyte/stainless steel cells at room temperature and monitored for 20 days. X-ray diffraction patterns of the prepared membranes were obtained by Rigaku miniflex diffractometer at room temperature. Surface morphology of the composite electrolytes was studied by using Scanning Electron Microscope (SEM) (JEOL 6390 LV). The size of PAni nanofibers was determined by TEM (JEOL-TEM-100 CXII).

4.2 Results and discussion

4.2.1 TEM studies

Fig. 2 shows the TEM micrograph of PAni nanofibers. From the figure it is observed that nanofiber is composed of randomly packed polymer chains. As the PAni nanofibers are

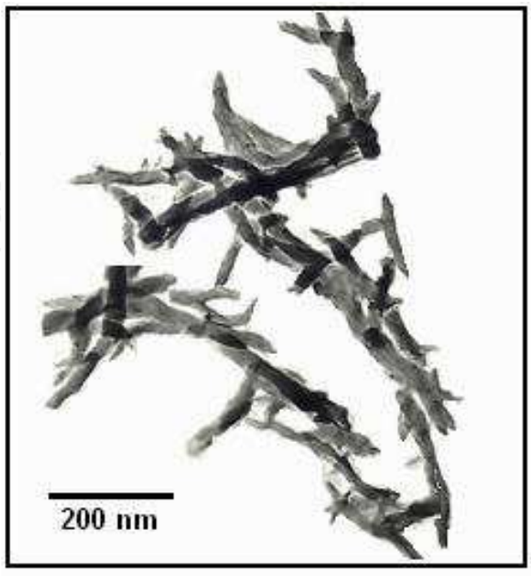

Fig. 2. TEM micrograph of dedoped Pani nanofibers

synthesized by interfacial polymerization, overgrowth of polyaniline on the nanofiber scaffolds does not take place and nanofibrillar morphological units are formed. The diameter and length of the fibers are found to be 20 nm to 30 nm and more than 1000 nm respectively. These high aspect ratio (> 50) nanofibers were used in polymer electrolytes as a filler to increase the ionic conductivity and electrochemical properties.

4.2.2 Ionic conductivity studies

Fig. 3a shows the impedance plot of P(VdF-HFP)-(PC+DEC)-$LiClO_4$ polymer electrolyte and Fig. 3b presents the complex impedance spectra of P(VdF-HFP)-(PC+DEC)-$LiClO_4$-x% dedoped polyaniline nanofiber (x = 2, 4, 6, 8 and 10) composite polymer electrolytes. The

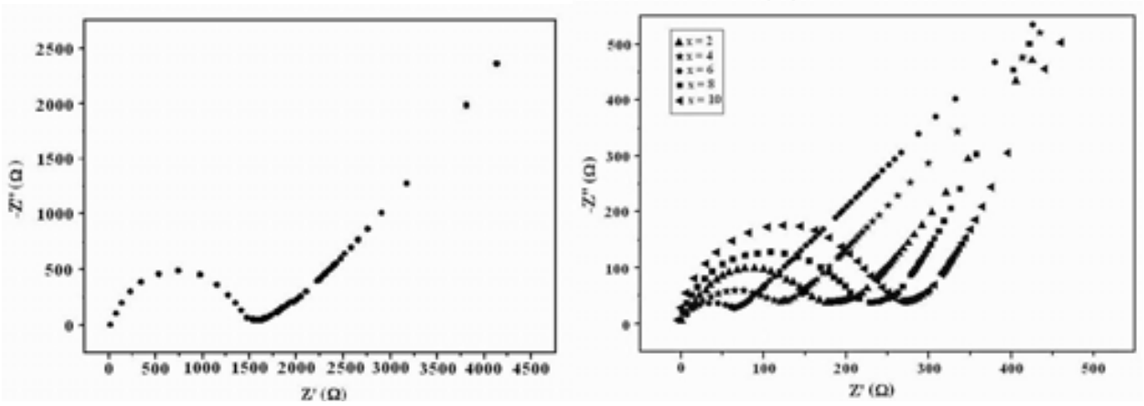

(a) (b)

Fig. 3. (a) Complex impedance spectrum of P(VdF-HFP)-(PC+DEC)-$LiClO_4$ gel polymer electrolyte without incorporating dedoped nanofibers.
(b) Complex impedance spectra of P(VdF-HFP)-(PC+DEC)-$LiClO_4$-x% dedoped polyaniline nanofibers (x = 2, 4, 6, 8 and 10)

impedance spectra comprise a distorted semicircular arc in the high frequency region followed by a spike in the lower frequency region (Aravindan & Vickraman, 2008). The high frequency semicircle is due to the bulk properties and the low frequency spike is due to the electrolyte and electrode interfacial properties. The impedance spectra can be modeled as an equivalent circuit having a parallel combination of a capacitor and a resistor in series or parallel with a constant phase element (CPE) (Marzantowicz et al., 2005). The impedance of CPE is given by

$$Z_{CPE} = k\,(j\omega)^{-p} \quad \text{where } 0 < p < 1 \tag{1}$$

When p=0, Z is frequency independent and k is just the resistance and when p=1, $Z = k/j\omega = -jk/\omega$, the constant k_1 now corresponds to the capacitance. When p is between o and 1, the CPE acts in a way intermediate between a resistor and a capacitor. The use of series CPE terms tilts the spike and parallel CPE terms depress the semicircle. The bulk electrical resistance value (R_b) is calculated from the intercept at high frequency side on the Z' axis. The ionic conductivity is calculated from the relation $\sigma = l/R_b r^2\pi$; where l and r are thickness of polymer electrolyte membrane and radius of the sample membrane discs and R_b is the bulk resistance obtained from complex impedance measurements. The value of σ_{ionic} of

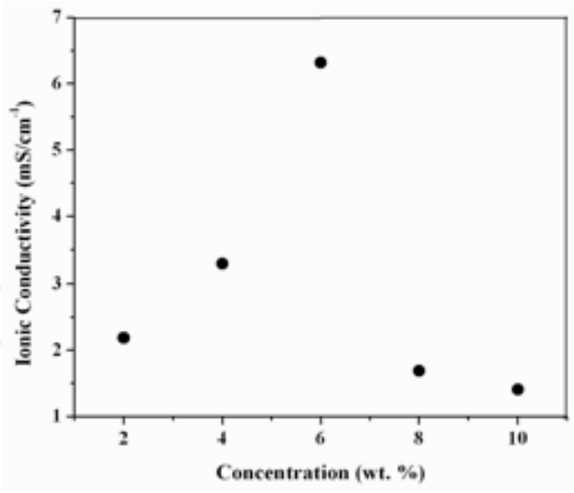

Fig. 4. Variation of ionic conductivity of P(VdF-HFP)-(PC+DEC)-$LiClO_4$-x% dedoped polyaniline nanofibers with nanofiber concentration.

plasticized nanocomposite polymer electrolytes was evaluated from complex impedance spectra and expressed as a function of nanofiber concentration at room temperature (25°C) as shown in Fig. 4. It is observed that the σ_{ionic} increases with increase in nanofiber concentration. Maximum conductivity was found to be 6.31 $\times 10^{-3}$ Scm^{-1} at room temperature for x = 6 wt. % dedoped polyaniline nanofiber filler, which is by over one order of magnitude higher as compared to that (2.5×10^{-4} Scm^{-1}) for polymer electrolyte without nanofibers. However as the filler (dedoped nanofiber) concentration increases beyond 6 wt. %, the ionic conductivity decreases. It is known that plasticized polymer electrolytes show highly porous structure created by plasticized rich phase (Aravindan & Vickraman, 2007). When dedoped polyaniline nanofiber is incorporated in the porous membrane, the movement of Li^+ ion through the pores is facilitated by the filler due to formation of conduction path resulting in higher conductivity. As the nanofiber content increases from 2 wt. % to 6 wt. % the porous structure is remarkably widened leading to entrapment of large volume of liquid electrolyte in the pores, which results in increase in ionic conductivity. Moreover the reorganization of P(VdFHFP) chains is prevented due to high aspect ratio (> 50) nanofibers leading to increase in amorphicity with increasing concentration of nanofibers which is consistent with XRD results. However, XRD results show that beyond 6 wt. % the nanofibers get phase separated out from the polymer matrix and form insulating aggregation (Wieczorek et al., 1996), which impede the Li^+ ion motion resulting in decrease in ionic conductivity. Fig. 5 shows the conductivity versus temperature inverse plots of polymer electrolyte membranes in the temperature range from 25°C to 60°C. Highest ionic conductivity of 2.2 $\times$ 10^{-2} Scm^{-1} has been found at 60°C with 6 wt. % of dedoped polyaniline nanofibers. The figure shows that the ionic conduction in nanocomposites polymer electrolytes obey the Vogel-Tamman-Fulcher (VTF) relation (Quartarone et al., 1998)

$$\sigma = \sigma_0 \exp(-B/k(T-T_0)) \quad (2)$$

where B is a constant with dimensions that of the energy, T_0 is the idealized glass transition temperature at which the probability of configurational transition tends to become zero and is generally regarded as having a value between 20 to 50 K below glass transition

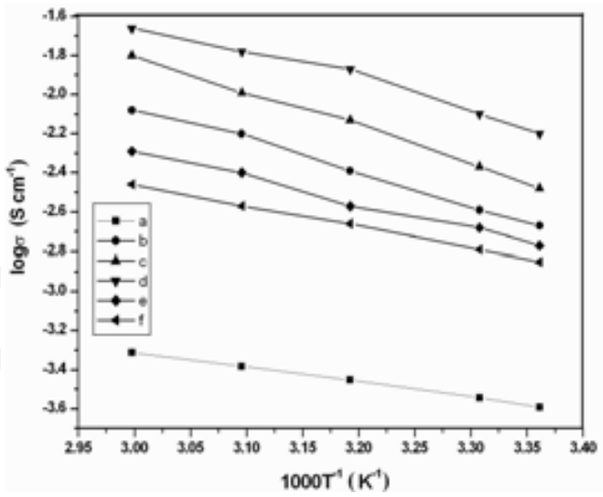

Fig. 5. Logσ vs. temperature inverse curves of P(VdF-HFP)-(PC+DEC)-$LiClO_4$-x% dedoped polyaniline nanofibers membranes (a) x=0, (b) x=2, (c) x=4, (d) x=6, (e) x=8, (f) x=10.

temperature (T_g) of the polymer. Since T_g of P(VdF-HFP) is -100°C, T_0 will be far below the temperature regions of measurements from room temperature (25°C) to 60°C. Therefore, VTF behavior (2) can be modeled as Arhenius behavior as shown lnσ vs. 1000/T plots in Fig. 5. As expected the increase in temperature leads to increase in ionic conductivity because as the temperature increases the polymer expands to produce more free volume, which leads to enhanced ionic mobility and polymer segmental mobility. The enhancement of ionic conductivity by the dedoped polyaniline nanofiber can be explained by the fact that the nanofiber inhibits the recrystallization kinetics, helping to retain the amorphous phase down to relatively low temperatures (Rhoo et al., 1997).

4.2.3 Interfacial stability

Compatibility of nanocomposites polymer electrolyte with electrode materials is an important factor for polymer battery applications. In order to improve the interfacial stability of polymer electrolytes before and after incorporating dedoped polyaniline nanofiber, the ionic conductivity was measured by fabricating stainless steel/polymer electrolyte membrane/stainless steel cells at room temperature and monitored for 20 days. Polymer electrolytes without nanofiber and containing 6 wt. % of dedoped polyaniline nanofiber have been selected to observe the effect of nanofiber on interfacial stability and the results are shown in Fig. 6.

It reveals that ionic conductivity of both the electrolytes decreased with time but decrease of ionic conductivity in the polymer electrolyte without nanofiber is much larger as compared to that of polymer electrolytes containing nanofibers. This result confirms that the interfacial stability of the polymer electrolyte containing nanofibers is better than that of without nanofibers. This can be attributed to the fact that when nanofiber is added passivation of polymer electrolyte due to reaction with electrode material decreases. High aspect ratio (> 50) nanofibers get accumulated on the surface of the electrode and effectively impede the electrode electrolyte reaction (Zhang et al., 2004). Fig. 7 schematically depicts that when dedoped (insulating) nanofibers are incorporated in the polymer electrolyte the electrolyte does not make direct contact with the electrode, which increases the interfacial stability.

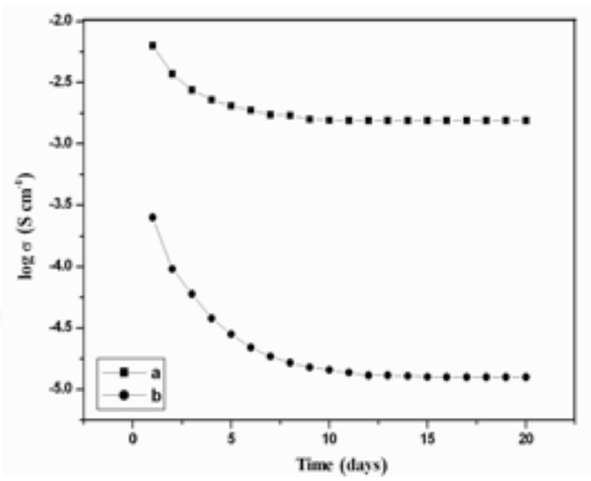

Fig. 6. Interfacial stability of (a) P(VdF-HFP)-PC+DEC-$LiClO_4$-6% dedoped polyaniline nanofibers polymer electrolyte and (b) P(VdF-HFP)-PC+DEC-$LiClO_4$ gel polymer electrolyte

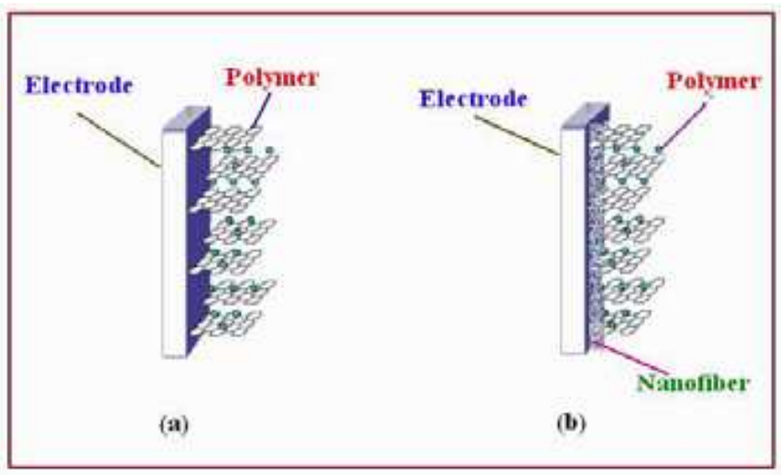

Fig. 7. Schematic representation of electrode/polymer electrolyte interfacial passivation (a) without and (b) with dedoped polyaniline nanofibers. without nanofibers

4.2.4 XRD analysis

X-ray diffraction patterns of pure P(VdF-HFP) and dedoped polyaniline nanofibers are presented in Fig. 8(a & b). In Fig. 8a the peaks at $2\theta=20^o$ and 38° correspond to (020) and (202) crystalline peaks of P(VdF) (Abbrent et al, 2001). This is a confirmation of partial crystallization of the PVdF units in the copolymer to give an overall semi-crystalline morphology for P(VdF-HFP). High intensity peaks at $2\theta=20^o$ and $2\theta=23^o$ are observed in the XRD pattern of dedoped polyaniline nanofiber (Fig. 8b). Fig. 9(a-f) shows the XRD patterns of P(VdF-HFP)-(PC+DEC)-$LiClO_4$-x% dedoped polyaniline nanofiber composite polymer electrolytes. It is observed that the addition of dedoped polyaniline nanofibers in polymer electrolytes increases the broadening and decreases the intensity of XRD peaks. This is due to fact that addition of nanofibers prevents polymer chain reorganization causing significant disorder in the polymer chains which promotes the interaction between them (Kumar et al., 2007).

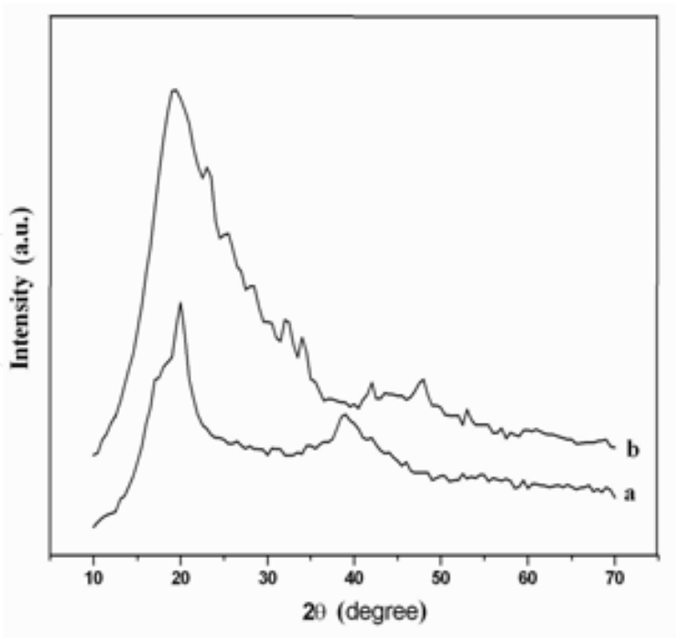

Fig. 8. XRD patterns of pure (a) P(VdF-HFP) and (b) Dedoped polyaniline nanofibers.

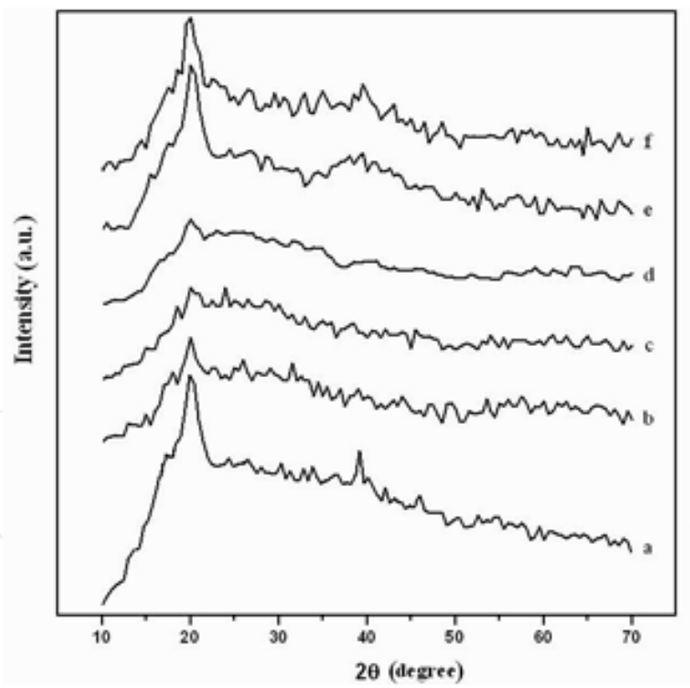

Fig. 9. XRD patterns of P(VdF-HFP)-(PC+DEC)-$LiClO_4$-x% dedoped polyaniline nanofibers membranes (a) x=0, (b) x=2, (c) x=4, (d) x=6, (e) x=8, (f) x=10.

4.2.5 Morphological study

Scanning electron micrographs of P(VdF-HFP)-(PC+DEC)-$LiClO_4$-x% dedoped polyaniline nanofiber gel composite polymer electrolytes are shown in Fig. 10(a-f). It is observed that the

polymer electrolytes show highly porous structure with uniform pore distribution. Addition of fillers (dedoped polyaniline nanofibers) resulted in improved morphology, since the fillers occupied the pores along with the plasticizers. It is observed that pore distribution on the surface of the polymer electrolytes becomes denser with the increase of filler (dedoped polyaniline nanofibers) content at first, and reaches the maximum when the weight ratio of filler is about 6 wt. % (Fig. 10d), subsequently decreases when filler content increases further {Fig. 10(e-f)}. In composite gel polymer electrolytes the porous structure gives conducting pathways for Li^+ movement (Arvindan & Vickraman, 2007). The high aspect ratio of nanofibers remarkably increases the pore density and widens the porous structure of the polymer electrolytes (Xi et al., 2006). The above phenomenon is possibly due to the fact that the dedoped nanofibers try to occupy the pores in the gel polymer electrolyte and in the process pore distribution becomes denser. Highly porous structure leads to better connectivity of the liquid electrolyte through the pores accounting for the increase in ionic conductivity. Highly porous surface morphology of the polymer electrolytes is effectively formed on account of the interaction of dispersed dedoped (insulating) nanofibers with polymer component as well as the affinity with solvent molecules (Kim et al., 2003). However beyond 6 wt. % of filler content the nanofibers get phase separated from the P(VdF-HFP) matrix and form insulating clusters. These phase separated insulating percolation clusters impede ion movement and hence ionic conductivity decreases. The phenomenon of phase separation is strongly supported by XRD results as discussed in section 3.4.

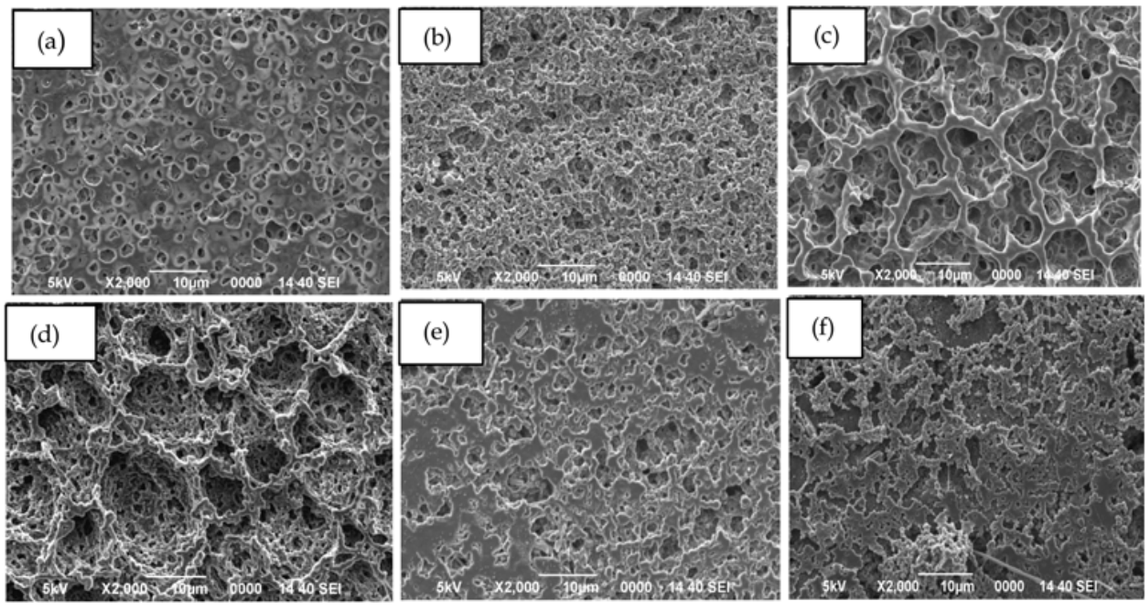

Fig. 10. SEM micrographs of P(VdF-HFP)-(PC+DEC)-$LiClO_4$-x% dedoped polyaniline nanofibers membranes (a) x=0, (b) x=2, (c) x=4, (d) x=6, (e) x=8, (f) x=10.

4.2.6 FTIR studies

FTIR is a powerful tool to characterize the chain structure of polymers and has led the way in interpreting the reactions of multifunctional monomers including rearrangements and isomerizations (Pavia et al., 2001). FTIR spectra of P(VdF-HFP), $LiClO_4$, dedoped polyaniline

nanofibers and polymer complexes are shown in Fig. 11. The symmetric and asymmetric C-H stretching vibration of pure P(VdF-HFP) is observed at 3000cm^{-1}. Frequency 1633 cm^{-1} is assigned to C=O, C=C bonding. Frequencies 1486 cm^{-1} and 1404 cm^{-1} are assigned to $-CH_3$ asymmetric bending and C–O stretching vibration of plasticizer propylene carbonate and diethyl carbonate. Frequencies 12861066 cm^{-1} are assigned to –C–F– and $-CF_2-$ stretching vibration. Frequency 881 cm^{-1} is assigned to vinylidene group of polymer. The vibrational peaks of PVdF and $LiClO_4$ are shifted to (1786, 1401, 882, 837 cm^{-1}) and (1633, 1154, 626 cm^{-1}) in the polymer electrolyte respectively. The C–N stretching vibration of secondary amine in polyaniline nanofiber arises at 1289 cm^{-1}. The ammonium ion displays broad absorption in the frequency region 33503050 cm^{-1} because of N-H stretching vibration. The N-H bending vibration of secondary aromatic amine of polyaniline nanofiber occurs at 1507 cm^{-1}. The

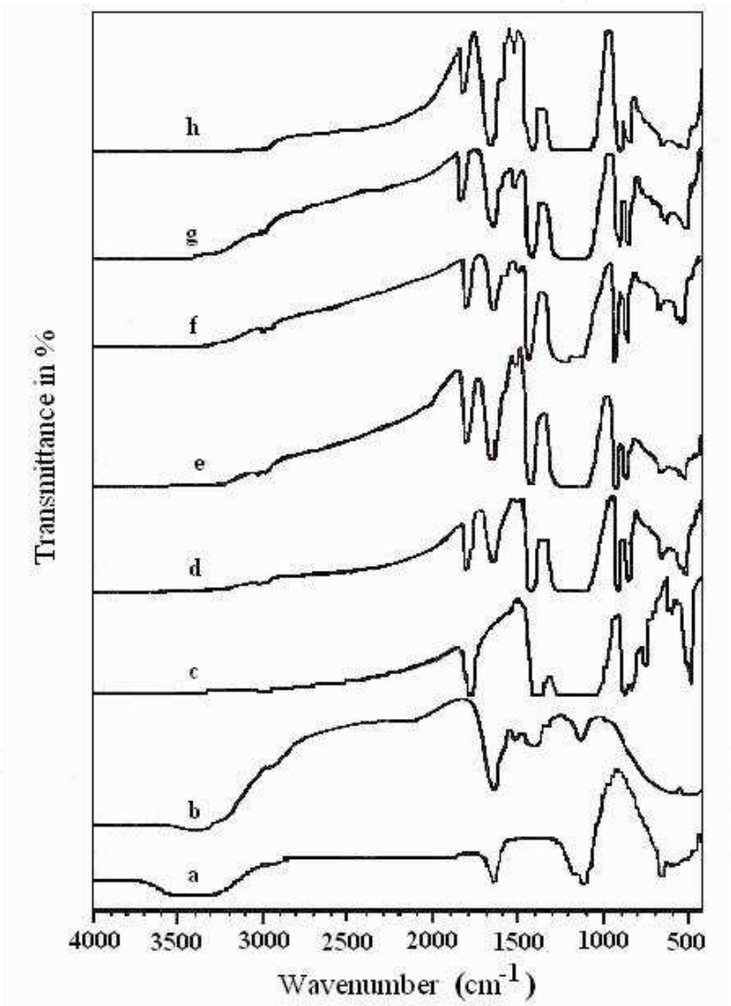

Fig. 11. FTIR spectra of (a) $LiClO_4$, (b) dedoped polyaniline nanofibers, (c) P(VdF-HFP), (d) P(VdF-HFP)-(PC+DEC)-$LiClO_4$-2% dedoped polyaniline nanofibers, (e) P(VdF-HFP)-(PC+DEC)-$LiClO_4$-4 % dedoped polyaniline nanofibers, (f) P(VdF-HFP)-(PC+DEC)-$LiClO_4$-6 % dedoped polyaniline nanofibers, (g) P(VdF-HFP)-(PC+DEC)-$LiClO_4$-8 % dedoped polyaniline nanofibers, (h) P(VdF-HFP)-(PC+DEC)-$LiClO_4$-10 % dedoped polyaniline nanofibers composite polymer electrolyte systems.

frequency 1637 cm^{-1} of polyaniline nanofiber is assigned to C=C of aromatic ring. As mentioned earlier the C-H symmetric and asymmetric bending frequencies are observed at 3000 cm^{-1} in pure P(VdF-HFP). However, after incorporating dedoped polyaniline nanofibers the corresponding bands in the electrolyte systems show a large shift (3021 cm^{-1}) in higher frequency region which is a characteristic of highly disordered conformation (Porter et al., 1987). This is in good agreement with the XRD results.

5. PEO/P(VdF-HFP)-$LiClO_4$-Dedoped polyaniline nanofibers composite solid polymer electrolyte system:

5.1 Preparation

The host polymer PEO (M_W = 6, 00,000), the copolymer P(VdF-HFP) (M_W = 4,00,000) and salt lithium perchlorate ($LiClO_4$) were received from Aldrich, USA. All the raw materials were heated at 50 °C under vacuum. Organic solvents acetonitrile and acetone were used as received from Emerk to prepare thin polymer electrolyte membranes by solution casting technique. Appropriate amount of PEO and salt $LiClO_4$ (O/Li = 8) were dissolved in acetonitrile and then mixed together, stirred and heated at 50 °C. P(VdF-HFP) was fixed at 40 wt. % of PEO for all samples, was stirred in presence of acetone at 50 °C. Subsequently both the polymer solutions were mixed, stirred and heated at 50 °C for 12-14 hours. Dedoped polyaniline nanofibers were then added in the blend polymer solutions and allowed to stir for another 7-8 hours. The viscous solution thus obtained was cast onto Petri dish and allowed to dry at room temperature. This procedure provided mechanically stable, free standing and flexible membranes. The blend based composite polymer electrolyte membranes used in this study were denoted as PEO-$LiClO_4$-P(VdF-HFP)-x% dedoped polyaniline nanofibers (x = 0, 5, 10, 15, 20, 25).

5.2 Results and discussion

5.2.1 X-Ray diffraction studies

X-ray diffraction patterns of pure PEO, P(VdF-HFP) and dedoped polyaniline nanofibers are presented in Fig. 12(a-c). High intensity peaks at $2\theta=20^o$ and $2\theta=23^o$ are observed in the XRD pattern of dedoped polyaniline nanofibers. In Fig. 12b the peaks at $2\theta=20^o$ and 38° correspond to (020) and (202) crystalline peaks of P(VdF-HFP). PEO shows a characteristic peak at $2\theta=20^o$. Fig. 13 shows the XRD patterns of PEO-P(VdF-HFP)-$LiClO_4$-x% dedoped polyaniline nanofibers composite polymer electrolytes. It is observed that when P(VdF-HFP) is blended with PEO, no additional peak appears, only the intensity of crystalline peaks decreases suggesting that the amorphicity increases (Leo et al., 2002). When dedoped polyaniline nanofibers are incorporated in the PEO-P(VdF-HFP)-$LiClO_4$ the intensity further decreases as shown in Fig. 13(b-f). The degree of crystallinity is determined by a method described elsewhere (Saikia et al., 2006). It is observed that the degree of crystallinity decreases with increasing nanofibers concentration and reaches a minimum at 15 wt. % nanofibers concentration. This reduction in crystallinity upon addition of nanofibers is attributed to the suppression of the reorganization of polymer chains by the nanofibers (Scrosati et al., 2001). However, at higher concentration of nanofibers (>15 wt.%), the degree of crystallinity increases with increasing nanofibers concentration indicating that crystalline phase starts increasing above 15 wt.% of nanofibers concentration due to reorganization of polymer chains in PEO-P(VdF-HFP)-$LiClO_4$ electrolyte system. At 20 wt.% and 25 wt.% of nanofibers concentration an additional peak appears at $2\theta=23^o$, which can be assigned to

dedoped polyaniline nanofibers suggesting that above 15 wt.% polyaniline nanofibers get phase separated from the PEO-P(VdF-HFP)-$LiClO_4$ polymer electrolyte phase.

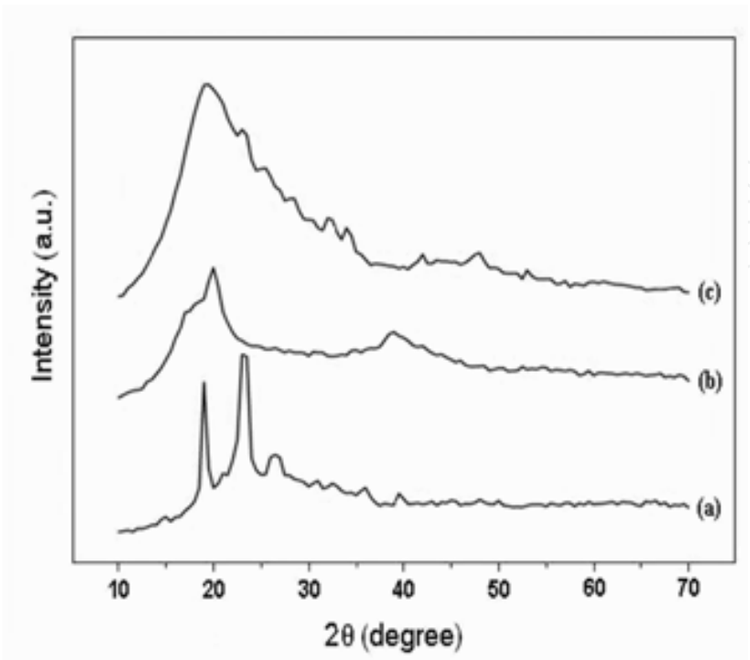

Fig. 12. XRD patterns of (a) PEO, (b) P(VdF-HFP), (c) dedoped polyaniline nanofibers.

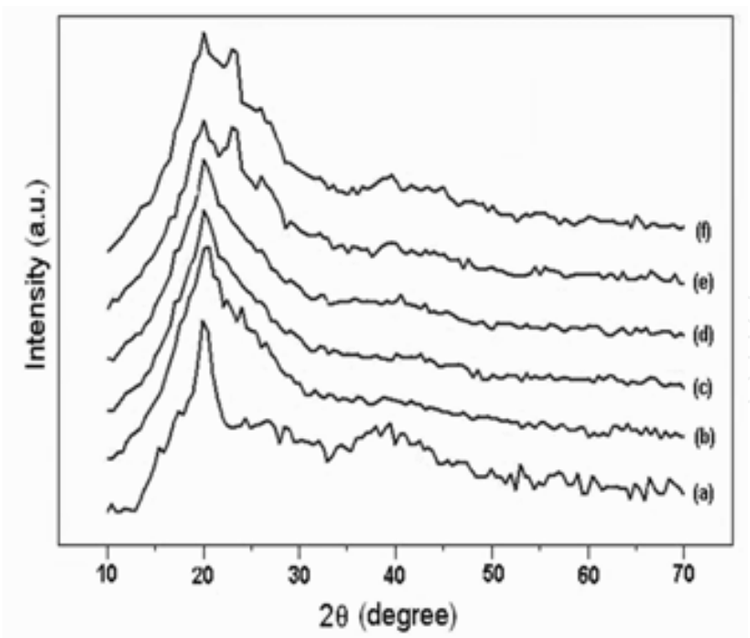

Fig. 13. XRD patterns of PEO-P(VdF-HFP)-$LiClO_4$-x% dedoped polyaniline nanofibers polymer electrolyte membranes (a) x = 0, (b) x = 5, (c) x = 10, (d) x = 15, (e) x = 20 and (f) x = 25.

5.2.2 Ionic conductivity studies

The complex impedance plots for PEO-P(VdF-HFP)-$LiClO_4$ polymer electrolyte membranes with different concentration of polyaniline nanofibers are presented in Fig. 14(a-f). The variation of ionic conductivity with increasing concentration of nanofibers is shown in Fig. 15. It is observed that the σ_{ionic} increases with increase in concentration of nanofibers. Maximum conductivity was found to be 3.1×10^{-4} Scm^{-1} at room temperature for 15 wt. % dedoped polyaniline nanofiber fillers, which is over seven times higher as compared to that (4.5×10^{-5} Scm^{-1}) for polymer electrolyte without nanofibers. However, as the filler (dedoped nanofibers) concentration increases beyond 15 wt. %, the ionic conductivity decreases. The enhancement up to 15 wt. % of nanofibers concentration seems to be correlated with the fact that the dispersion of dedoped polyaniline nanofibers to PEO-P(VdF-HFP) prevents polymer chain reorganization due to the high aspect ratio (>50) of nanofibers, resulting in reduction in polymer crystallinity, which gives rise to an increase in ionic conductivity. The increase in ionic conductivity may also result from Lewis acid-base interaction (Rajendran & Uma, 2000; Croce et al., 2001; Chung et al., 2001, Stephan & Nahm, 2006). In the present composite polymer electrolytes, the oxygen atom in PEO has two lone pair of electrons and nitrogen atom in PAni nanofibers has one lone pair of electrons, which act as strong Lewis base centers and Li^+ cations as strong Lewis acid giving rise to numerous acid-base complexes in the composite polymer electrolyte. This allows mobile ions to move more freely either on the surface of the nanofibers or through a low density polymer phase at the interface, which results in enhanced ionic conductivity. The reduction in crystallinity upon addition of polyaniline nanofibers up to 15 wt. % is consistent with XRD results. Enhancement in ionic conductivity can also be attributed to the creation of polymer-filler interface. The filler-polymer interface is a site of high defect concentration providing channels for faster ionic transport (Kumar & Scanlon, 1994) and the structure and chemistry of filler-polymer interface may have even more important role than the formation of amorphous phase in the electrolyte.

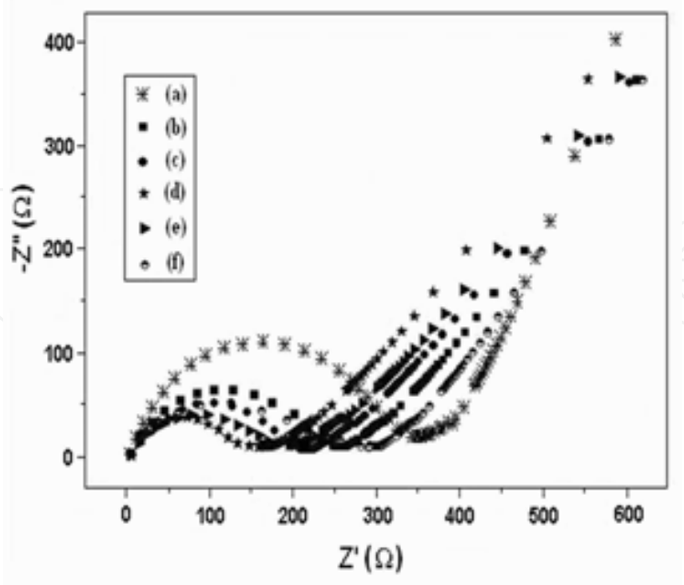

Fig. 14. Complex impedance spectra of PEO-P(VdF-HFP)-$LiClO_4$-x% dedoped polyaniline nanofibers polymer electrolyte membranes (a) x = 0 (b) x = 5, (c) x = 10, (d) x = 15, (e) x = 20 and (f) x = 25.

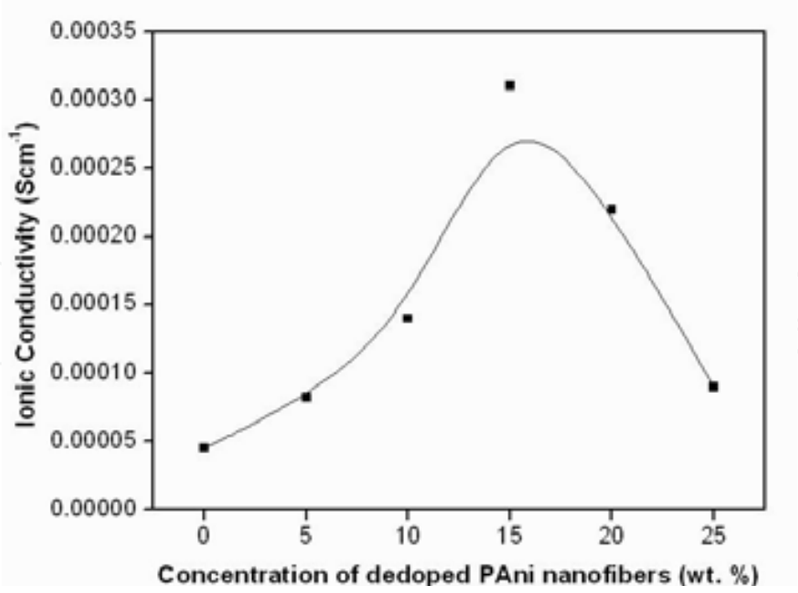

Fig. 15. Variation of ionic conductivity with different concentration of dedoped polyaniline nanofibers.

On the other hand, the decrease in ionic conductivity for concentration of nanofibers higher than 15 wt. % can be attributed to the blocking effect on the transport of charge carriers resulting from the phase separation of nanofibers (Kim & Park, 2007). Besides, above 15 wt. % of nanofibers concentration a depressed semicircle is seen in the impedance spectra, which is characteristic of a system where more than one conduction processes are present simultaneously (Kurian et al., 2005). SEM micrographs show that, at higher concentration of nanofibers (15 wt. %), a two phase microstructure is observed. This could be attributed to the fact that at higher concentration of nanofibers, uniform dispersion of nanofibers in PEO-P(VdF-HFP) matrix is difficult to achieve due to formation of phase-separated morphologies. This is expected to affect the conductivity of the system, since a large concentration of Li^+ cations are trapped in the phase separated nanofibers. Thus the decrease of ionic conductivity above 15 wt. % nanofibers content can be attributed to the effect of phase separation, which is consistent with the XRD and SEM results. Fig. 16 shows the conductivity versus temperature inverse plots of polymer electrolyte films in the temperature range from 25°C to 80°C. All the samples show a break point at around 60 °C, near the melting temperature of PEO, reflecting the well-known transition from PEO crystalline to amorphous phase.

As expected the increase in temperature leads to increase in ionic conductivity because as the temperature increases the polymer chains flex at increased rate to produce larger free volume, which leads to enhanced polymer segmental and ionic mobilities. The enhancement of ionic conductivity by the dedoped polyaniline nanofibers can be explained by the fact that the nanofibers inhibit the recrystallization kinetics, helping to retain the amorphous phase down to relatively low temperatures (Rhoo et al, 1997).

5.2.3 Morphological studies

The SEM micrographs for PEO-P(VdF-HFP)-$LiClO_4$-x% dedoped polyaniline nanofibers membranes are presented in Fig. 17(a-f). In general three-four phases are known to coexist

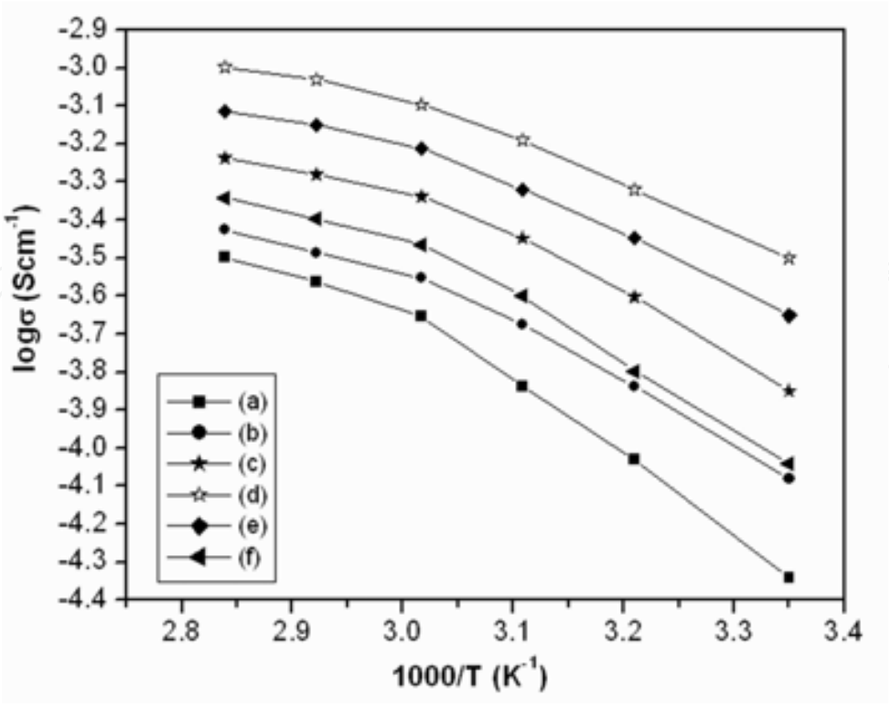

Fig. 16. logσ vs. temperature inverse curve PEO-P(VdF-HFP)-$LiClO_4$-x% dedoped polyaniline nanofibers polymer electrolyte membranes (a) x = 0, (b) x = 5, (c) x = 10, (d) x = 15, (e) x = 20 and (f) x = 25

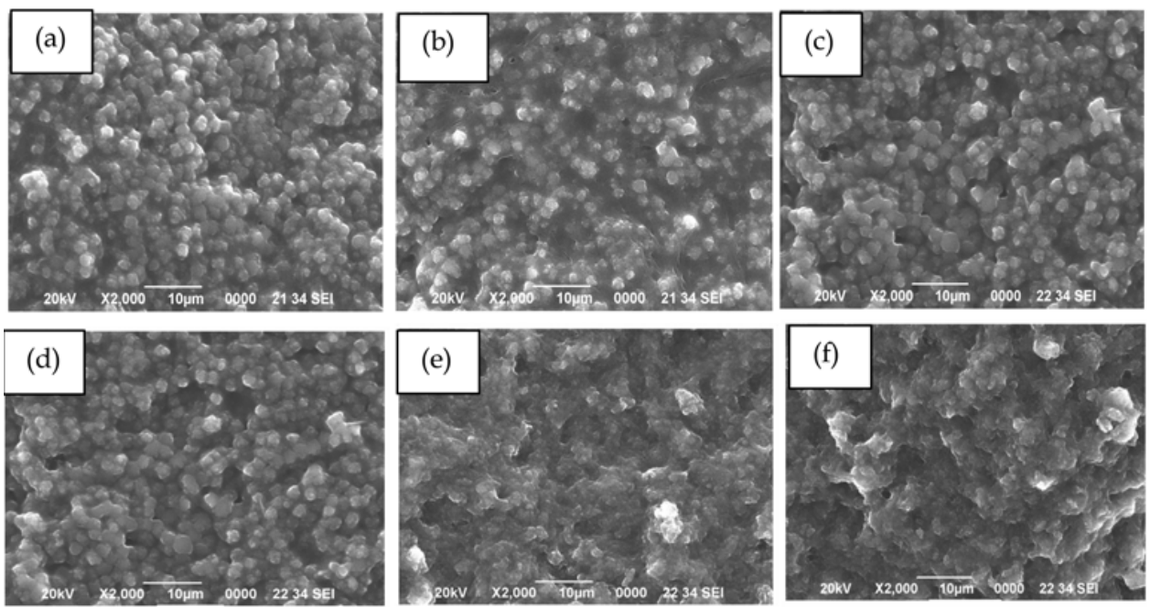

Fig. 17. SEM micrographs of PEO-P(VdF-HFP)-$LiClO_4$-x% dedoped polyaniline nanofibers polymer electrolytes (a) x = 0, (b) x = 5, (c) x = 10, (d) x = 15, (e) x = 20 and (f) x = 25.

in the PEO based polymer electrolytes viz. crystalline PEO phase, crystalline PEO-Li salt complex phase and amorphous PEO phase. It is observed that below 15 wt. % nanofibers

concentration (Fig. 17a-c), the surface morphology is granular and smooth, which could be attributed to the reduction of PEO crystallinity due to complexation with lithium salt and polyaniline nanofibers. At 15 wt% concentration of nanofibers, rough morphology and sharp interfaces are observed (Fig. 17d) which may facilitate lithium ion conduction along the interface (Saikia & Kumar, 2005).
Fig. 17e shows that at 20 wt% of nanofiber concentration a two phase microstructure is observed due to phase segregation of nanofibers. Phase separation becomes more prominent at 25 wt% of nanofibers as shown in Fig. 17f. The nanofibers get phase separated from the PEO-P(VdF-HFP) polymer matrix and form domain like regions, which may act as physical barriers to the effective motion of the ions leading to decrease in ionic conductivity.

6. Conclusions

Stable dedoped PAni nanofiber-P(VdF-HFP) composites can be readily prepared by interfacial polymerization followed by solution casting method. The TEM result shows that polyaniline nanofibers of diameter 20-30 nm in size are formed by interfacial polymerization. The ionic conductivity of dedoped PAni nanofiber-P(VdF-HFP) based composite electrolyte was influenced by increase in PAni content. It obeys the Arrhenius Law of conductivity. The dedoped PAni nanofiber-P(VdF-HFP) based composite electrolyte has the highest ionic conductivity of 6.3×10^{-3} Scm $^{-1}$ at room temperature. The crystallinity is found to decrease in case of composites. Increase in ionic conductivity can be attributed to the fact that dispersed nanofibers improve the porous structure of the gel polymer electrolytes forming better connectivity for ion motion through the liquid electrolyte. This is confirmed by SEM results. However at higher filler content conductivity decreases because the dedoped nanofibers start forming insulating clusters that encumber ion movement. The interfacial stability of the nanofibers dispersed polymer gel electrolyte membranes is observed to be better than that of gel polymer electrolytes without nanofibers. XRD analysis reveals that amorphicity increases upon addition of nanofibers which could be attributed to the reduction in chain reorganization of polymer by nanofibers.
In the PEO-P(VdF-HFP)-$LiClO_4$ polymer electrolyte the XRD, SEM and conductivity results show that the conductivity of increases when dedoped polyaniline nanofibers are added as a filler upto a concentration of 15 wt%. At higher concentration (> 15 wt%) the polyaniline nanofibers get phase separated from the polymer matrix. The three moieties PEO, P(VdF-HFP) and dedoped polyaniline nanofiber no longer remain a miscible uniform phase but nanofibers get phase separated.
Both the electrolyte systems show that by using dedoped (insulating) polyaniline nanofibers as fillers the ionic conductivity can be enhanced. It is also observed that there is a certain critical concentration above which the dedoped polyaniline nanofiber phase gets separated out from the electrolyte which thereby reduces the ionic conductivity. A probable explaination for this effect can be stated as when the concentration of the dedoped nanofibers is increased agglomeration occurs, the nanofiber phase gets separated out from the electrolyte and some domain like structures are formed which is evident from the SEM images. These domain like structures caused due to the increase in concentration of the dedoped nanofibers create barriers in the conducting path and hinders the ionic movement thereby reducing the ionic conductivity.

7. References

Abbrent, S.; Plestil, J.; Hlavata, D.; Lindgren, J.; Tegenfeldt, J. & Wendsjo, A. (2001). Crystallinity and morphology of PVdF-HFP-based gel electrolytes. *Polymer*, 42, 1407-1416.

Abraham, K.M. (1993). Highly conductive polymer electrolytes, In: *Applications of electroactive polymers*, Scrosati, B. (Ed.), 75-112, Chapman and Hall, London.

Ahn, J.-H. ; Wang, G.X.; Liu, H.K. & Dou, S.X. (2003). Nanoparticle-dispersed PEO polymer electrolytes for Li batteries. *J Power Sources*, 119121, 422-426.

Algamir, M. & Abraham, K.M. (1994). Lithium batteries, new materials, developement and prospectives, In: *Industrial chemistry library*, *vol. 5*, Pistoia, G. (Ed.), 93-136, Elsevier, Amsterdam.

Appetecchi, G.B.; Crose, F. & Scrosati, B. (1995). Kinetics and stability of the lithium electrode in poly(methylmethacrylate)-based gel electrolytes. *Electrochim. Acta*, 40, 991-997.

Aravindan, V. & Vickraman, P. (2007). Polyvinylidenefluoride-hexafluoropropylene based nanocomposite polymer electrolytes(NCPE) complexed with $LiPF_3(CF_3CF_2)_3$. *Eur. Polym. J* 43, 5121-5127.

Aravindan, V. & Vickraman, P. (2008). Characterzation of SiO_2 and Al_2O_3 incorporated PVdF-HFP based composite polymer electrolytes with $LiPF_3(CF_3CF_2)_3$. *JAppl. Polym. Sci.*, 108, 1314-1322.

Bhattarai, S.R.; Bhattarai, N.; Yi, H.K.; Hwang, P.H., Cha, D.I. & Kim, H.Y. (2004). Novel biodegradable electrospun membrane: scaffold for tissue engineering. *Biomaterials*, 25, 2595–2602.

Carrière, D.; Barboux, P.; Chaput, F.; Spalla, O. & Boilot J. P. (2001). Enhanced connectivity in hybrid polymers. *Solid State Ionics*, 145,141-147.

Chatterjee, A. & Deopura, B.L. (2002). Carbon nanotubes and nanofibre: an overview. *Fiber Polym.*, 3(4), 134–139.

Chen, H. W.; Chiu, C.Y.; Wu, H.D.; Shen, I.W. &. Chang, F.C. (2002). Solid state electrolyte nanocomposites based on poly (ethylene oxide), poly (oxypropelene) diamine, mineral clay and lithium perchlorate. *Polymer*, 43, 5011-5016.

Choe, H.S.; Giaccami, J.; Alamgir, M. & Abraham, K.M. (1995). Preparation and characterization of poly(vinyl sulfone)- and poly(vinylidene fluoride)- based electrolytes. *Electrochim. Acta*, 40, 2289-2293.

Chronakis, I. S. (2005). Novel nanocomposites and nanoceramics based on polymer nanofibers using electrospinning process—a review. *J. Mater. Process. Technol.* 167, 283-293.

Chung, S.H.; Wang, Y.; Persi, L.; Croce, F.; Greenbaum, S.G.; Scrosati, B. & Plichta, E. (2001). Enhancement of ion transport in polymer electrolytes by addition of nano-scale inorganic oxides. *J Power Sources* 97-98, 644-648.

Croce, F.; Appetecchi, G.B.; Persi, L. & Scrosati, B. (1998). Nanocomposite polymer electrolytes for lithium batteries. Nature, 394, 456-458.

Croce, F.; Persi, L.; Scrosati, B.; Serraino-Fiory, F.; Plichta, E. & Hendrickson, M.A. (2001). Role of the ceramic fillers in enhancing the transport properties of composite polymer electrolytes. *Electrochim. Acta*, 46, 2457-2461.

De Heer, W.A.; Bacsa, W.S.; Chatelain, A.; Gerfin, T.; Humphrey-Baker, R.; Forro, L. & Ugarte, D. (1995). Aligned nanotube films: production and optical and electronic properties. *Science*, 268:845-847.

Delvaux, M.; Duchet, J.; Stavaux, P.-Y.; Legras, R. & Demoustier-Champagne, S. (2000). Chemical and electrochemical synthesis of polyaniline micro- and nano-tubules. *Synth. Met.*, 113, 275280.

Dzenis, Y. (2004). Spinning continuous fibers for nanotechnology. *Science*, 304, 1917-1919.

Fenton, B.E.; Parker, J.M. & Wright, P.V. (1973). Complexes of alkali metal ions with poly(ethylene oxide). *Polymer*, 14, 589.

Feuillade, G. & Perche, Ph. (1975). Ion-conductive macromolecular gels and membranes for solid lithium cells. *J Appl. Electrochem.*, 5, 6369.

Goel, S.; Mazumdar, N.A. & Gupta A. (2009). Synthesis and characterization of polypyrrole nanofibers with different dopants. *Polymers for Advanced Technologies*, DOI: 10.1002/pat.1516.

Golodnitsky, D.; Ardel, G. & Peled, E. (2002). Ion-transport phenomena in concentrated PEO-based composite polymer electrolytes. Solid State Ion. 147, 141-155.

Gray, F.M. (1991). *Solid polymer electrolytese fundamental and technological applications*, VCH, London, NewYork.

He, X.; Shi, Q.; Zhou, X.; Wan, C. & Jiang, C. (2005). In situ composite of nano SiO2 -P(VDF-HFP) porous polymer electrolytes for Li-ion batteries; *Electrochim. Acta*, 51,1069-1075.

Huang, J. (2006). Syntheses and applications of conducting polymer polyaniline nanofibers. *Pure Appl. Chem.*, 78, 15-27.

Huang, Z. -M.; Zhang, Y. Z.; Kotaki, M. & Ramakrishna, S. (2003). A review on polymer nanofibers by electrospinning and their applications in nanocomposites. *Compos. Sci. Technol.* 63, 2223-2253.

Jacob, M.M.E.; Hackett, E. & Giannelis, E.P. (2003). From nanocomposite to nanogel polymer electrolytes. *J Mater. Chem.* 13, 1-5.

Kalyana Sundaram, N.T.; Vasudevan, T. & Subramania A. (2007). Synthesis of ZrO_2 nanoparticles in microwave hydrolysis of Zr (IV) salt solutions—Ionic conductivity of PVdF-co-HFP-based polymer electrolyte by the inclusion of ZrO_2 nanoparticles. *Journal of Physics and Chemistry of Solids*, 68, 264-271.

Kim, K.M.; Ko, J. M.; Park, N. –G.; Ryu, K. S. & Chang, S. H. (2003). Characterization of poly(vinylidenefluoride-co-hexafluoropropylene)-based polymer electrolyte filled with rutile TiO_2 nanoparticles. *Solid State Ionics*, 161(1-2), 121-131.

Kim, K.M.; Park, N.-G. ; Ryu, K.S. & Chang, S.H. (2002). Characterization of poly(vinylidenefluoride-co-hexafluoropropylene)-based polymer electrolyte filled with TiO_2 nanoparticles. *Polymer*, 43, 3951-3957.

Kim, K.M.; Ryu, K.S.; Kang, S. –G.; Chang, S. H. & Chung, I. J. (2001). The effect of silica addition on the properties of poly(vinylidene fluoride)-co-hexafluoropropylene)-based polymereElectrolytes. *Macromol. Chem. Phys.*, 202(6), 866-872.

Kim, S. & Park, S.-J. (2007). Preparation and electrochemical behaviors of polymeric composite electrolytes containing mesoporous silicate fillers. *Electrochim. Acta* 52, 3477-3484.

Klein, J.D.; Herrick II, R.D.; Palmer, D.; Sailor, M.J.; Brumlik, C.J. and Martin, C.R. (1993). Electrochemical fabrication of cadmium chalcogenide microdiode arrays. *Chem. Mater.*, 5, 902-904.

Kovac, M.; Gaberscek, M. & Grdadolnik, J. (1998). The effect of plasticizer on the microstructural and electrochemical properties of a $(PEO)_nLiAl(SO_3\ Cl)_4$ system. Electrochim. Acta, 44, 863-870.

Kumar, B. & Scanlon, L.G. (1994). Polymerceramic composite electrolytes. *J Power Sources*, 52, 261-268.

Kumar, G. G.; Kim, P.; Nahm, K. S. & Elizabeth, R. N. (2007). Structural characterization of PVdF-HFP/ PEG/Al_2O_3 proton conducting membranes for fuel cells. *J Membr. Sci.*, 303,126-131.

Kumar, R.; Subramania, A.; Kalyana Sundaram, N.T.; Vijaya Kumar, G. & Bhaskaran, I. (2007). Effect of MgO nanoparticles on ionic conductivity and electrochemical properties of nanocomposite polymer electrolyte. *J Membr. Sci.*, 300, 104-110.

Kurian, M.; Galvin, M.E.; Trapa, P.E.; Sadoway, D.R. & Mayes, A.M. (2005). Singleion conducting polymer–silicate nanocomposite electrolytes for lithium battery applications. *Electrochim. Acta,* 50, 2125-2134.

Leo, C.J.; Rao, G.V.S. & Chowwdari, B.V.R. (2002). Studies on plasticized PEO–lithium triflate-ceramic filler composite electrolyte system. *Solid State Ionics*, 148, 159-171.

Lobitz, P.; Fullbier, H.; Reich, A. & Ambrahsat, K. (1992). Polymer solid electrolytes-PEO and alkali halides: A modified preparative technique. *Solid State Ionics*, 58, 49-54.

Ma, P.X. & Zhang, R. (1999). Synthetic nano-scale fibrous extracellular matrix. Synthetic nano-scale fibrous extracellular matrix. *J Biomed. Mater. Res.*, 46, 60–72.

Martin, C. R. (1994). Nanomaterials: A membrane-based synthetic approach. *Science* 266, 1961-1966.

Marzantowicz, M.; Dygas, J.R.; Jenninger, W. & Alig, I. (2005). Equivalent circuit analysis of impedance spectra of semicrystalline polymer. *Solid State Ionics*, 176, 2115-2121.

Michael, M.S. & Prabaharan, S.R.S. (2004). Rechargeable lithium battery employing a new ambient temperature hybrid polymer electrolyte based on PVK+PVdF–HFP (copolymer). *J Power Sources*, 136, 408-415.

Morales, A.M. & Lieber, C.M. (1998). A laser ablation method for the synthesis of crystalline semiconductor nanowires. *Science*, 279, 208-211.

Pathasarathy, R.V. & Martin, C.R.. (1994). Synthesis of polymeric microcapsule arrays and their use for enzyme immobilization. *Nature*, 369:298-301.

Pavia, D.L.; Lampman, G.M. & Kriz, G.S. (2001). *Introduction to spectroscopy*, third ed., Harcourt College Publ., USA.

Porter, M.D.; Bright, T.B.; Allara, D.L. & Chidsey, C.E.D. (1987). Spontaneously organized molecular assemblies. 4. Structural characterization of n-alkyl thiol monolayers on gold by optical ellipsometry, infrared spectroscopy, and electrochemistry. *JAm. Chem.Soc.*, 109, 3559-3568.

Quartarone, E.; Mustarelli, P. & Magistris, A. (1998). PEO-based composite polymer electrolytes. Solid State Ionics, 110, 1-14.

Rajendran, S.; Kannan, R. & Mohendran O. (2001). An electrochemical investigation on PMMA/PVdF blend-based polymer electrolytes. *Mater. Lett.*, 49, 172-179.

Rajendran, S. & Uma, T. (2000). Conductivity studies on PVC/PMMA polymer blend electrolyte. *Mater. Lett.*, 44, 242-247.

Rhoo, H.J.; Kim, H.T.; Park, J. M. & Hwang, T. S. (1997). Ionic conduction in plasticized PVC/PMMA blend polymer electrolytes. *Electrochim. Acta*, 42, 1571-1579.

Saikia, D.; Hussain, A.M.P.; Kumar, A.; Singh, F. and Avasthi, D.K. (2006). Ionic conduction studies in Li $^{3+}$ ion irradiated (PVDF-HFP)-(PC+DEC)-$LiCF_3SO_3$ gel polymer electrolytes. *NIMB*, 244, 230-234.

Saikia, D. & Kumar, A. (2005). Ionic transport in P(VDF-HFP)-PMMA-$LiCF_3SO_3$-(PC+DEC)-SiO_2 composite gel polymer electrolyte. *Eur. Polym. J*, 41, 563-568.

Scrosati, B.; Croce, F. & Panero, S. (2001). Progress in lithium polymer battery R&D. *J Power Sources*, 100, 93-100.

Scrosati, B.; Croce, F. & Persi L. (2000). Impedance spectroscopy study of PEObased nanocomposite polymer electrolytes. *J Electrochim Soc*, 147, 1718-1721.

Song, J.Y.; Wang, Y.Y. & Wan, C.C. (2000). Conductivity study of porous plasticized polymer electrolytes based on poly(vinylidene fluoride). A comparison with polypropylene separators. *J Electrochem. Soc.*, 147, 3219-3225.

Steinhart, M.; Wendolff, J. H.; Greiner, A., Wehrspohn, R. B.; Nielsch, K.; Choi, J. & Gosele, U. (2002). Polymer Nanotubes by Wetting of Ordered Porous Templates. *Science*, 296, 1997.

Stephan, A.M. & Nahm, K.S. (2006). Review on composite polymer electrolytes for lithium batteries. Polymer, 47, 5952-5964.

Stephan, A.M.; Nahm, K.S.; Kumar, T.P.; Kulandainathan, M.A.; Ravi, G. & Wilson, J. (2006). Nanofiller incorporated poly(vinylidene fluoride–hexafluoropropylene) (PVdF–HFP) composite electrolytes for lithium batteries. J. Power Sources, 159, 1316-1321.

Stephan, A. M.; Nahm, K. S.; Prem Kumar, T.; Kulandainathan, M. A.; Ravi, G. & Wilson, J. (2006). Nanofiller incorporated poly(vinylidene fluoride–hexafluoropropylene) (PVdF–HFP) composite electrolytes for lithium batteries; *J Power Sources*, 159,1316-1321.

Stephan, A.M.; Renganathan, N.G.; Kumar, T.P.; Pitchumani, R.; Shrisudersan, J. & Muniyandi, N. (2000). Ionic conductivity studies on plasticized PVC/PMMA blend polymer electrolyte containing $LiBF_4$ and $LiCF_3SO_3$. *Solid State Ionics*, 130, 123-132.

Stolarska, M.; Niedzicki, L.; Borkowska, R.; Zalewska, A. & Wieczorek, W. (2007) Structure, transport properties and interfacial stability of PVdF/HFP electrolytes containing modified inorganic filler. *Electrochim. Acta*, 53,1512-1517.

Subbiah, T.; Bhat, G.S.; Tock, R.W. Parameswaran, S. & Ramkumar, S.S. (2005). Electrospinning of nanofibers. *J Appl. Polym. Sci.* 96, 557–569.

Sundararajan, S.; Bhushan, B., Namazu, T. & Isono, Y. (2002). Mechanical property measurements of nanoscale structures using an atomic forcemicroscope. *Ultramicroscopy*, 91(1–4):111–118.

Suthar, A. & Chase, G. (2001). Nanofibres in filter media. *Chem. Eng.*, 726, 26–28.

Tarascon, J.-M.; Gozdz, A.S.; Schmutz, C.; Shokoohi, F. & Warren, P.C. (1994). Performance of Bellcore's plastic rechargeable Li-ion batteries. *Solid State Ionics*, 86, 49-54.

Taylor, G.I. (1969). Electrically driven jets. *Proc R. Soc. London*, Ser A, 313, 453-475.

Li, D. & Xia, Y. (2004). Electrospinning of nanofibers: Reinventing the wheel?. *Adv. Matter.*, 16, 1151-1170.

Van de Zande, B.M.I.; Bohmer, M.R.; Fokkink, L.G.J. & Shonenberger. C. (1997). Aqueous gold sols of rod-shaped particles. *J Phys. Chem.B*, 101, 852-854.

Wang, Z. & Tang, Z. (2004). A novel polymer electrolyte based on PMAML/PVDF-HFP blend. Electrochim. Acta, 49,1063-1068.

Wieczorek, W.; Stevens, J.R. & Florjanczyk, Z. (1996). Composite polymer based solid electrolytes. The Lewis acidbased approach. *Solid State Ionics*, 85, 67-72.

Wu, C.-G.; Lu, M.I.; Tsai, C.-C. & Chuang, H.-J. (2006). PVdF-HFP/ metal oxide nanocomposites: The matrices for highconducting, low-leakage porous polymer electrolytes. *J Power Sources*, 159, 295-300.

Xi, J.; Qiu, X.; Li, J.; Tang, X.; Zhu, W. & Chen, L. (2006). PVDFPEO blends based microporous polymer electrolyte: effect of PEO on pore configurations and ionic conductivity. *J Power Sources*, 157, 501-506.

Zhang, S.S.; Ervin, M.H.; Xu, K. & Jow, T.R. (2004). Microporous poly (acrylonitrile-methyl methacrylate) membrane as a separator of rechargeable lithium battery. *Electrochim. Acta*, 49, 3339-3345.

Zhang, Y.; Ouyang, H.; Lim, C.T.; Ramakrishnan, S. & Huang, Z.M. (2005). Electrospinning of gelatin fibers and gelatin/PCL composite fibrous scaffolds Electrospinning of gelatin fibers and gelatin/PCL composite fibrous scaffolds. *J Biomed. Mater. Res. Part B: Appl. Biomater.*, 72B, 156–165.

Nanofibers

Edited by Ashok Kumar

ISBN 978-953-7619-86-2
Hard cover, 438 pages
Publisher InTech
Published online 01, February, 2010
Published in print edition February, 2010

“There’s Plenty of Room at the Bottom” this was the title of the lecture Prof. Richard Feynman delivered at California Institute of Technology on December 29, 1959 at the American Physical Society meeting. He considered the possibility to manipulate matter on an atomic scale. Indeed, the design and controllable synthesis of nanomaterials have attracted much attention because of their distinctive geometries and novel physical and chemical properties. For the last two decades nano-scaled materials in the form of nanofibers, nanoparticles, nanotubes, nanoclays, nanorods, nanodisks, nanoribbons, nanowhiskers etc. have been investigated with increased interest due to their enormous advantages, such as large surface area and active surface sites. Among all nanostructures, nanofibers have attracted tremendous interest in nanotechnology and biomedical engineering owing to the ease of controllable production processes, low pore size and superior mechanical properties for a range of applications in diverse areas such as catalysis, sensors, medicine, pharmacy, drug delivery, tissue engineering, filtration, textile, adhesive, aerospace, capacitors, transistors, battery separators, energy storage, fuel cells, information technology, photonic structures and flat panel displays, just to mention a few. Nanofibers are continuous filaments of generally less than about 1000 nm diameters. Nanofibers of a variety of cellulose and non-cellulose based materials can be produced by a variety of techniques such as phase separation, self assembly, drawing, melt fibrillation, template synthesis, electro-spinning, and solution spinning. They reduce the handling problems mostly associated with the nanoparticles. Nanoparticles can agglomerate and form clusters, whereas nanofibers form a mesh that stays intact even after regeneration. The present book is a result of contributions of experts from international scientific community working in different areas and types of nanofibers. The book thoroughly covers latest topics on different varieties of nanofibers. It provides an up-to-date insightful coverage to the synthesis, characterization, functional properties and potential device applications of nanofibers in specialized areas. We hope that this book will prove to be timely and thought provoking and will serve as a valuable reference for researchers working in different areas of nanofibers. Special thanks goes to the authors for their valuable contributions.

How to reference

In order to correctly reference this scholarly work, feel free to copy and paste the following:

A. Kumar and M. Deka (2010). Nanofiber Reinforced Composite Polymer Electrolyte Membranes, Nanofibers, Ashok Kumar (Ed.), ISBN: 978-953-7619-86-2, InTech, Available from: http://www.intechopen.com/books/nanofibers/nanofiber-reinforced-composite-polymer-electrolyte-membranes

InTech Europe
University Campus STeP Ri
Slavka Krautzeka 83/A
51000 Rijeka, Croatia
Phone: +385 (51) 770 447
Fax: +385 (51) 686 166
www.intechopen.com

InTech China
Unit 405, Office Block, Hotel Equatorial Shanghai
No.65, Yan An Road (West), Shanghai, 200040, China
中国上海市延安西路65号上海国际贵都大饭店办公楼405单元
Phone: +86-21-62489820
Fax: +86-21-62489821

IntechOpen

IntechOpen